Thermochimica Acta, 67 (1983) 223–232
Elsevier Science Publishers B.V., Amsterdam – Printed in The Netherlands

THERMAL AND X-RAY STUDY OF SODIUM DEOXYCHOLATE CRYSTAL AND FIBRE

A.R. CAMPANELLI, D. FERRO, E. GIGLIO, P. IMPERATORI and V. PIACENTE
Istituto di Chimica Fisica, Università di Roma, 00185 Rome (Italy)

(Received 1 March 1983)

ABSTRACT

Sodium deoxycholate forms hexagonal crystals, macromolecular fibres and, in aqueous solution, micellar aggregates. All these phases show a close resemblance in the distribution of the X-ray intensities, so it is reasonable to suppose that they are composed of almost identical structural units. X-Ray and thermal measurements confirm that the crystal and the fibre present similar structures and vaporization behaviour, as well as practically the same enthalpy changes. These structural models are used and checked in the study of the micellar solutions.

INTRODUCTION

3α, 12α-Dihydroxy-5β-cholan-24-oic acid (deoxycholic acid, DCA) presents two faces, one polar with two secondary hydroxyl groups at C_3 and C_{12}, and the other apolar, with two angular methyl groups at C_{10} and C_{13} (see Fig. 1). This property is responsible for the ability of the DCA alkali-metal salts to form micellar aggregates in aqueous solutions [1]. The geometry of the DCA molecule and the deoxycholate anion (DC^-) is known from the determination of many crystal structures of DCA inclusion compounds [2] and a monoclinic phase of rubidium deoxycholate [3]. The crystal packings are characterized by two structural motifs, the bilayer and the helix, stabilized chiefly by hydrogen bonds.

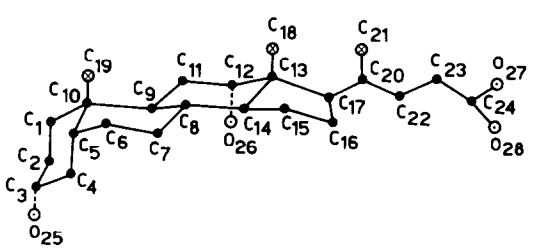

Fig. 1. Atomic numbering of DCA. Hydrogen atoms are omitted.

0040-6031/83/$03.00

The sodium salt of DCA (NaDC) is one of the most important bile salts since it is capable of solubilizing water-insoluble compounds [4–10], many of which are of biological interest, such as cholesterol [4,5], phospholipids [6], sequential copolypeptides [7], and tingenone [8]. By varying some thermodynamic parameters as, for example, ionic strength, pH, temperature and pressure, it is possible to increase the size of the NaDC micellar aggregates so as to obtain a gel composed of helical macromolecules [11,12]. Fibres can be drawn from NaDC aqueous solutions which give rise to a detailed X-ray diffraction pattern [11]. This pattern can be interpreted in terms of a hexagonal lattice in which the steroid molecules are probably arranged in helices. On ageing, the fibres change into hexagonal crystals of NaDC (space group $P6_1$ or $P6_5$), also obtainable by crystallizing NaDC from water or from a mixture of water and acetone. The structural motif in the crystal is the helix, formed by NaDC molecules, held together mainly by hydrogen bonds and coulombic interactions among Na^+ and DC^- ions and water molecules. Since the X-ray intensity distributions of the NaDC aqueous solutions, fibres and crystals are similar, it is reasonable to suppose that the micellar aggregates are also helical, at least within a concentration range far from the critical micellar concentration. This hypothesis is in disagreement with the model of the "primary" and "secondary" micelles proposed for NaDC [13] and currently accepted.

In order to verify the similarity of the structure among crystals, fibres, and micelles we have undertaken a thermal, vaporization and X-ray study of these phases. In the present work the results concerning the crystals and the fibres are reported.

EXPERIMENTAL

Materials

NaDC purchased from Calbiochem was crystallized from a mixture of water and acetone and its purity was confirmed by thin layer chromatography. Hexagonal crystals were obtained with a NaDC: H_2O ratio of 1 : 4, and their composition was established by X-ray, density, spectropolarimetric, thermogravimetric and elemental analysis measurements. No acetone was detected by NMR spectra. Fibres were prepared by adding 0.015 M hydrogen iodide to a 0.1 M NaDC aqueous solution. The solution was drawn out into glassy and brittle fibres. I^- was oxidized to I_2 and removed from the solution by means of oxygen to prevent the presence of sodium iodide in the fibres, which showed the same composition of the crystals.

METHODS

The X-ray data of NaDC crystals and fibres were recorded, using CuK_α radiation, by means of Weissenberg, precession and Debye–Scherrer cameras. The intensities of a NaDC hexagonal single crystal were collected up to $2\theta = 110°$ by the ω-scan mode on a Syntex $P2_1$ automated diffractometer with graphite-monochromatized CuK_α radiation. 3234 independent reflections with $I > 3\sigma(I)$ were observed.

The density was measured by suspending the samples in a mixture of cyclohexane–carbon tetrachloride. Subsequently the density of the mixture was determined by means of a DMA O2C densimeter.

The melting points were measured at atmospheric pressure by means of a Leitz 350 heating plate.

Thermal scans were accomplished by means of a DuPont 990 thermal analyzer and 951 thermobalance, using heating rates of 10°C min^{-1} and 2°C min^{-1} for the DSC and TGA measurements, respectively.

The pressure of the vapour in equilibrium with the solid NaDC was measured by the torsion effusion method [14]. The employed assembly has been described previously [15]. The vapour pressures of the compound at each experimental temperature were derived from measurements of the torsion angle, α, of the cell using the relation

$$P = 2K\alpha/(a_1 l_1 f_1 + a_2 l_2 f_2)$$

where K is the constant of the torsion wire ($K = 0.346$ dyne cm rad^{-1}), a_1 and a_2 are the areas of the effusion holes, l_1 and l_2 are the respective distances from the rotation axis, and f_1 and f_2 are the corresponding geometrical factors evaluated from the equation [16]

$$1/f = 0.0147(R/r)^2 + 0.3490(R/r) + 0.9982$$

where R and r are the thickness and the radius of the effusion hole, respectively.

TABLE 1

Physical constants of the used torsion-effusion cells

	Semicell	Cell A (graphite)	Cell B (graphite)	Cell C (pyrophillite)	Cell D (glass)
Orifice area $\times 10^{-3}(\pm 0.05)$ [a] (cm^2)	1	2.83	12.23	12.30	~ 0.50
	2	2.83	12.23	12.30	~ 0.50
Force correction factors [16]	1	0.430	0.627	0.791	[b]
	2	0.430	0.620	0.792	[b]
Moment arm (± 0.05) (cm)	1	0.74	0.81	0.89	[b]
	2	0.77	0.79	0.85	[b]

[a] Measured by photographic enlargement.

[b] The constant $(1.09 \pm 0.10)10^{-4}$ kPa deg^{-1} of cell D was indirectly derived by vaporizations of standard elements.

Four different cells were used and their constants are given in Table 1. The operating cell temperature was measured by a calibrated chromel–alumel thermocouple placed inside an identical cell directly beneath the operating cell. As a check on the reliability of the pressure results, the vapour pressure of pure zinc was determined by using the different cells. From least-squares treatment of the measurements and their thermodynamic elaboration, the second- and third-law heat of vaporization of zinc was derived. The obtained values are in good agreement with that selected by Hultgren et al. [17]. The use of cells with different orifice areas and R and r values showed no dependence of the measured pressure, confirming the assumption that equilibrium conditions exist in the used torsion-effusion cells.

The vaporization behaviour of NaDC was investigated by heating accurately known amounts of the samples in well degassed glass crucibles inserted in a TECAM SBL-1 thermostatic fluidized sand bath and weighing the residues at different stages of the vaporization.

RESULTS

X-Ray analysis

Colourless prismatic crystals of NaDC, elongated along the c axis, were obtained from a mixture of water and acetone by cooling at 273 K. The unit cell constants are reported in Table 2. Patterson analysis and packing considerations supplied strong evidence for the occurrence of identical helices around the 6_1 (or 6_5) and 3_1 (or 3_2) screw axes. Thus, the asymmetric unit is composed of 3 NaDC and 12 H_2O molecules. One NaDC belongs to the 6_1 (or 6_5) helix, whereas the other two are adjacent molecules of the 3_1 (or 3_2) helix, which holds the six-fold symmetry. These findings were supported by a minimum residual analysis carried out computing the agreement index as a function of seven translational and rotational degrees of freedom. Six NaDC molecules are packed in 11.75 Å along c and have their C_9–C_{13} middle points about 8.6 Å from the helical axis (see Fig. 2). The interior of the helix is very likely filled with Na^+ ions and water molecules, which can stabilize the helix by means of ion–ion and ion–dipole interac-

TABLE 2

Crystallographic data of NaDC crystals and fibres

	a(Å)	b(Å)	c(Å)	α(°)	β(°)	γ(°)	Space group	d_x(g cm^{-3})	d_m(g cm^{-3})	M.p. (K)
Crystal	34.56	34.56	11.75	90	90	120	$P6_1$ or $P6_5$	1.20 [a]	1.208	574–576
Fibre	36.2	36.2	51.4	90	90	120		1.20 [b]	1.200	566–568

[a] Value calculated for 18 NaDC and 72 H_2O molecules in the unit cell.

[b] Value calculated for 87 NaDC and 348 H_2O molecules in the unit cell.

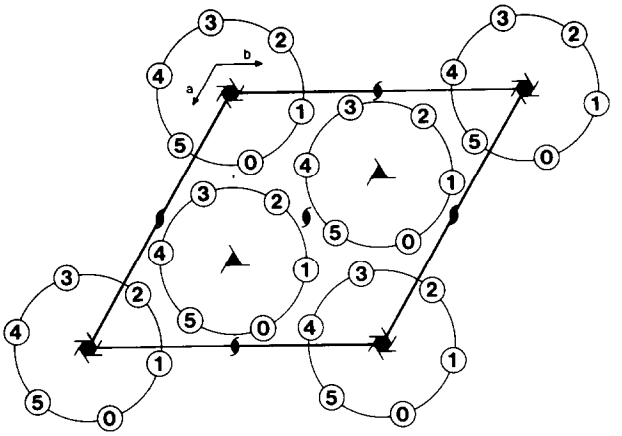

Fig. 2. Schematic drawing of the NaDC crystal packing viewed along c in the space group $P6_1$. The open circle and the figure inside it represent a DC^- and its height on c in $c/6$ units, respectively.

tions and hydrogen bonds. The 3_1 (or 3_2) helix can be obtained by rotating about 10° counter-clockwise and then by translation of $2/3$ a and $1/3$ b the 6_1 (or 6_5) helix. Work is in progress to establish the crystal structure at atomic resolution.

The X-ray pattern of the fibre fits a hexagonal cell with the dimensions reported in Table 2. The equatorial spacings are approximately equal to those of the crystal, so it is reasonable to suppose a similar packing of helices in the crystal and in the fibre. However, a comparison of the c values clearly indicates that the helix is different in the two phases. The value of c slightly differs from that given by Rich and Blow [11] (49.2 Å) and, moreover, no splitting of the fourth layer line was observed.

The three intense layer lines near the meridian, which occur at spacings of about 7.4, 6.4 and 5.7 Å, correspond to the seventh, eighth and ninth layer line, respectively, whereas a strong arc at 3.42 Å can belong to the 15th layer line. Thus, the helix, formed by 29 (NaDC + 4 H_2O) in order to agree with the observed density, can be generated by rotating 62.07° and by translating 1.77 Å a NaDC molecule. These values are nearly equal to the corresponding ones of 30 (NaDC + 4 H_2O), 60° and 1.96 Å found in the crystal, and justify the easy fibre → crystal transition by ageing. Further work is in progress to determine the macromolecular structure and packing of the fibre, very similar to that of the crystal (see Fig. 2).

Vaporization behaviour

The vaporization behaviour of NaDC crystals and fibres was studied by heating samples under vacuum ($\sim 10^{-6}$ atm) or at room pressure. The

experiments were carried out by vaporizing the samples at constant temperature for 30–180 min. In both pressure conditions, up to about 318–343 K the samples lost 16.4 ± 1.2% of their original weight. When the residues were heated up to about 530 K their weight loss is very small (~ 0.3%). Over this temperature the residues show rapid vaporization.

These results are substantially confirmed by TG measurements obtained by vaporizing NaDC crystals and fibres; as an example a typical TG plot of NaDC crystals is shown in Fig. 3. The weight loss of the samples in the first step of the vaporization can be explained by the loss of four crystallization water molecules (14.8%). Since the residues, placed in saturated water atmosphere, retake their original weight, the difference of about 1.6% in the weight loss is probably due to a degassing of the superficially adsorbed water. The presence of four water molecules was also confirmed by X-ray and density measurements.

The X-ray patterns of the residues of the first step of vaporization are like those of an amorphous structure; when the samples are again saturated by water, these show their original crystal structure. It was also noted that when NaDC crystal samples are heated at about 500 K a thin crust, probably due to a surface sinterization, is formed and prevents adsorption as well as evaporation of the water of crystallization.

Finally, the DSC thermal analysis performed during the vaporization of NaDC crystals and fibres within the temperature range 298–553 K showed similar behaviour of both compounds (see Fig. 4).

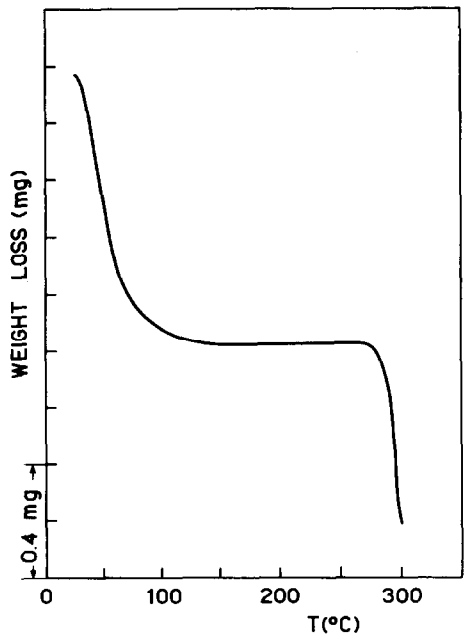

Fig. 3. TG plot of of NADC crystals (6.5 mg).

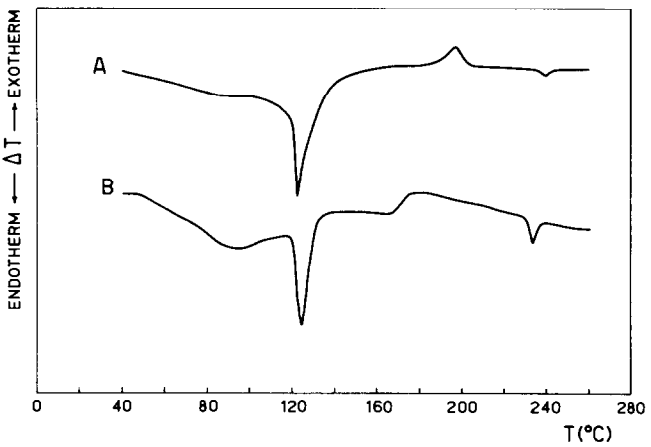

Fig. 4. DSC of NaDC. A, Crystals; B, fibres.

It is interesting to note that the endothermic peak at about 393 K corresponds to water evaporation and in the temperature range 443–493 K an exothermal process, probably due to reorganization of the solid phase, is broader in the fibre than in the crystal because of the more disordered structure of the fibres.

Vapour pressure measurements

Four vaporization runs of NaDC crystals and fibres were carried out. In the first step of the heating of the samples the pressure of the water of crystallization was measured. Only the first pressure data, when the sample has lost about 4–6% of the original weight, are reproducible. Thus, taking into account only these vapour pressure values, the following average pressure–temperature equation associated with the vaporization of the water of crystallization was derived from least-squares treatment of the data

$$\log P(\text{kPa}) = (9.02 \pm 0.38) - (3888 \pm 121)/T$$

The errors are standard deviations. The experimental values are reported in Fig. 5. In the experiments in which graphite cells were used, on increasing the temperature the torsion of the cells occurred at about 435 K (see Fig. 6) and the measured pressures and their dependence on the temperature are reproducible. Weighing the sample together with the graphite cell before and after the first step of the vaporization (up to 350 K) it was noted that the weight loss is about 7–9%. By heating the system up to 460 K it again loses 5–7% of the original weight. This can be explained by considering partial adsorption of the water in the graphite wall during the first step and the subsequent evaporation at 430–450 K. Considering the reproducibility of the phenomenon, from the temperature dependence of the vapour data the

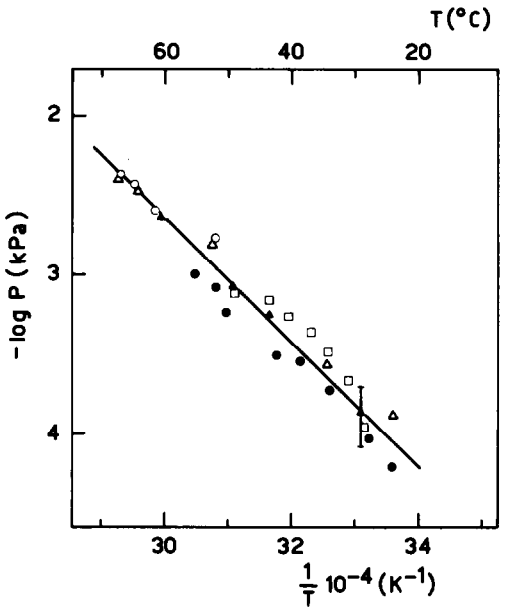

Fig. 5. Crystallization water pressure over NaDC crystal and fibre. Crystal: ▲ (cell A), △ (cell B), □ (cell C), ○ (cell D); fibre: ● (cell B).

vaporization enthalpy $\Delta H^0_{440} = 51 \pm 8$ kJ mole^{-1}, associated with the vaporization of water adsorbed in the graphite, was derived. This value agrees well enough with the bonding energies of less than about 0.5 eV reported by

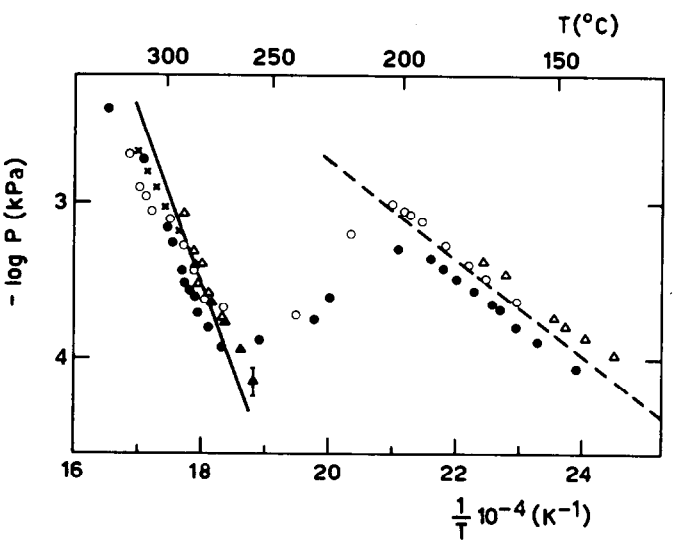

Fig. 6. Vapour pressure of the dehydrated NaDC crystal and fibre. Crystal: △ (cell B), ○ (cell A), ▲ (cell C), × (cell D); fibre: ● (cell B); ———— pure DCA (see ref. 19).

Hagstrum [18] for the physisorption of the adsorbate on the substrate due to Van der Waal's interactions.

When the pyrophillite and the glass cells were used the adsorption phenomenon was not noted. When the dehydrated NaDC samples were heated, a rapid increase in vapour pressure was observed at about 525 K (see Fig. 6). The temperature dependence of the vapour pressure can be expressed by the average equation

$$\log P(\text{kPa}) = (14.97 \pm 0.90) - (10015 \pm 400)/T$$

where the uncertainties are the standard deviations. This equation is similar to that found during the study of pure DCA [19]

$$\log P(\text{kPa}) = (16.16 \pm 0.24) - (10930 \pm 190)/T$$

CONCLUSION

The results indicate a close similarity between the structure of the NaDC crystal and that of the fibre. The X-ray data indicate that these two phases have the same monomeric unit, NaDC + 4 H_2O, which gives rise to two helices, one in the crystal and the other in the fibre, strictly related to each other. Both types of helix pack together with a nearly identical geometry, so the existence of the same inter- and intrahelical interactions can be supposed. This hypothesis is supported by the characteristic vaporization and DSC data which show a very similar behaviour of the two phases, mainly in the enthalpy changes due to the water release.

Vapour pressure data obtained in the first step of the vaporization permit a second-law enthalpy of the vaporization of the water of crystallization to be derived, $\Delta H^0_{318} = 74 \pm 6$ kJ mole^{-1}, where the associated error was estimated taking into account essentially the uncertainties in the temperature measurements.

It is interesting to note that while the pure deoxycholic acid at about 460–470 K loses $11 \pm 2\%$ of its original weight, probably due to a CO_2 molecule vaporization [19], its sodium salt does not present any evident weight loss within this temperature range. This may be explained by the occurrence of strong coulombic interactions between Na^+ and $-COO^-$ groups, which can further stabilize the carboxylic group as compared with the situation in the DCA inclusion compounds. On increasing the temperature the vaporization behaviour of dehydrated NaDC is similar to pure DCA [19].

ACKNOWLEDGEMENT

This work was sponsored by the Italian Consiglio Nazionale delle Ricerche—Progetto Finalizzato Chimica Fine e Secondaria.

NOTE ADDED IN PROOF

The space group of the NaDC crystal has now been determined as $P6_5$.

REFERENCES

1 D.M. Small, in P.P. Nair and D. Kritchevsky (Eds.), The Bile Acids, Plenum Press, New York, 1971, Ch. 8, pp. 249–356.
2 E. Giglio, J. Mol. Struct., 75 (1981) 39.
3 V.M. Coiro, E. Giglio, S. Morosetti and A. Palleschi, Acta Crystallogr., Sect. B, 36 (1980) 1478.
4 D.M. Small, M. Bourges and D.G. Dervichian, Nature (London), 211 (1966) 816.
5 M. Bourges, D.M. Small and D.G. Dervichian, Biochim. Biophys. Acta, 144 (1967) 189.
6 J. Philippot, Biochim. Biophys. Acta, 225 (1971) 201.
7 E. Corsi, M. D'Alagni and E. Giglio, Polymer, 17 (1976) 259.
8 A.R. Campanelli, M. D'Alagni, E. Giglio and G.B. Marini-Bettolo, Farmaco Ed. Prat., 36 (1981) 30.
9 K. Fontell, Kolloid Z.Z. Polym., 250 (1972) 333.
10 D.C. Thomas and S.D. Christian, J. Colloid Interface Sci., 82 (1981) 430.
11 A. Rich and D.M. Blow, Nature (London), 182 (1958) 423.
12 D.M. Blow and A. Rich, J. Am. Chem. Soc., 82 (1960) 3566.
13 D.M. Small, S.A. Penkett and D. Chapman, Biochim. Biophys. Acta, 176 (1969) 178.
14 R.D. Freeman, in J.L. Margrave (Ed.), The Characterization of High Temperature Vapour, Wiley, New York 1967.
15 V. Piacente and G. De Maria, Ric. Sci., 39 (1969) 549.
16 R.D. Freeman and A.W. Searcy, J. Chem. Phys., 22 (1954) 762.
17 R. Hultgren, R.L. Orr and K.K. Kelley, Selected Values of Thermodynamic Properties of Metals and Alloys, Wiley, New York, 1963.
18 H.D. Hagstrum, in H.L. Anderson (Ed.), AIP 50th Anniversary Physics, Vade Mecum, Am. Inst. Phys., New York, 1981.
19 D. Ferro, C. Quagliata, E. Giglio and V. Piacente, J. Chem. Eng. Data, 26 (1981) 192.